Available online at www.sciencedirect.com
ScienceDirect
Journal of Sound and Vibration 323 (2009) 974–988
JOURNAL OF SOUND AND VIBRATION
www.elsevier.com/locate/jsvi

Vibration analysis of rectangular plates with side cracks via the Ritz method

C.S. Huang[a,*], A.W. Leissa[b]

[a]Department of Civil Engineering, National Chiao Tung University, 1001 Ta-Hsueh Rd., Hsinchu 30050, Taiwan
[b]Department of Mechanical Engineering, Colorado State University, Fort Collins, CO 80523, USA

Received 15 May 2008; received in revised form 30 December 2008; accepted 8 January 2009
Handling Editor: L.G. Tham
Available online 12 February 2009

Abstract

This analysis deals with free vibrations of a rectangular plate with a side crack by using the famous Ritz method with special displacement functions. To appropriately describe the stress singularities at the crack tip and show the discontinuities of displacement and slope crossing the crack, previously used corner functions, as well as a new set of functions, are added to the well known admissible functions consisting of regular polynomials. Comprehensive convergence studies on the vibrations of simply supported rectangular plates with horizontal cracks at the symmetry axis are carried out and show that both the corner functions and the proposed new set of functions indeed accelerate the convergence of numerical solutions. Furthermore, the new set of functions is found to be particularly capable in improving convergence of solutions, especially when there is a large crack. Convergence studies also demonstrate that the present approach gives more accurate results than previously published approaches using the Ritz method combined with various domain composition techniques. Finally, the present approach is applied to investigate the effects of location, length and orientation of side cracks on the free vibration frequencies and mode shapes of simply supported and completely free square plates with side cracks, including cracks which are not along a symmetry axis, are skewed. Most of the results shown are novel.

1. Introduction

The flat plate is a very common component in engineering practices and has been extensively used in civil, mechanical and aerospace structures, such as concrete floor slabs and rudimentary surfaces for aircraft and guided missiles. The literature of free vibrations of plates is vast. Leissa [1] described about 500 publications which appeared before 1966, and more than 1500 papers have been published since then. Relatively few published results are available for cracked rectangular plates, and most of them considered plates with simply supported boundary conditions at all sides or at two opposite sides. Because exact analytical solutions exist for such plates with no crack, semi-analytical solutions can be constructed for such plates with cracks along a straight line perpendicular to the simply supported edges.

*Corresponding author.
E-mail addresses: cshuang@mail.nctu.edu.tw (C.S. Huang), awleissa@mindspring.com (A.W. Leissa).

0022-460X/$ - see front matter © 2009 Elsevier Ltd. All rights reserved.
doi:10.1016/j.jsv.2009.01.018

To investigate the vibrations of simply supported rectangular plates with cracks, Lynn and Kumbasar [2] used Green's functions to represent the transverse displacements of the plates, resulting in homogeneous Fredholm integral equations of the first kind, while Stahl and Keer [3] formulated such problems as dual series equations which reduced to homogeneous Fredholm integral equations of the second kind. Aggarwala and Ariel [4] applied Stahl and Keer's approach to analyze the vibration of a plate with various crack configurations along its symmetry axes. Neku [5] modified Lynn and Kumbasar's approach [2] by establishing the needed Green's functions via Levy's form of solution. Solecki [6] constructed a solution for vibrations of a cracked plate by using the Navier form of solution, along with finite Fourier transformation of discontinuous functions for the displacement and slope across the crack. Recently, Khadem and Rezaee [7] used so-called modified comparison functions constructed from Levy's solution as the admissible functions of the Ritz method to analyze a simply supported rectangular plate with a crack having an arbitrary length, depth and location parallel to one side of the plate. It should be noted that the approach of Khadem and Rezaee [7] can only be applied to deal with the rectangular plates with two opposite edges simply supported because of their special way of constructing admissible functions. Hirano and Okazaki [8] also developed solutions for vibrations of cracked rectangular plates with two opposite edges simply supported by utilizing Levy's form of solution and further matching the boundary conditions by means of a weighted residual method.

To consider the vibrations of a cracked rectangular plate with arbitrary boundary conditions, a numerical method has to be used. Both the finite element method and Ritz method have been often used. Qian et al. [9] developed a finite element solution by deriving the stiffness matrix for an element including the crack tip from the integration of the stress intensity factor. Krawczuk [10] proposed a solution similar to that of Qian et al. [9], except that the stiffness matrix for an element including the crack tip was expressed in a closed form. Yuan and Dickinson [11] decomposed a rectangular plate into several domains and introduced artificial springs at the interconnecting boundaries between the domains so that the Ritz method with regular admissible functions can be applied to find the solutions. Similar to the approach used by Yuan and Dickinson [11], Liew et al. [12] required the continuities of displacement and slope in a sense of integration along the interconnecting boundaries. In the approach of Liew et al. [12], the continuities of displacement and slope are not satisfied at every point along the interconnecting boundaries. Notably, the solutions of Yuan and Dickinson [11] and Liew et al. [12] destroy the good characteristics of providing upper-bound solutions for vibration frequencies, normally associated with the Ritz method.

In the above-mentioned literature, the solutions, except for the finite element solutions, by no means considered the characteristic of the stress singularities at the crack tip. The present work uses the well known Ritz method, considering also the stress singularities, to investigate the vibrations of side-cracked rectangular thin plates. The Ritz method is very suitable for solving the present problems because the geometry of plate under consideration is simple, so that the area integration required in the Ritz method is easy to set up.

The admissible functions to be used for solving the present problems include two sets of functions. One set is the well-known regular polynomials, which form a mathematically complete set of functions if an infinite number of terms are used. The other set of functions supplements the polynomials to appropriately describe the stress singularity behavior at the crack tip, as well as the possible discontinuities of displacement and slope across the crack. Since a crack is a special case of a V-notch, the asymptotic solutions (or corner functions) derived by Williams [13] would seem to be good candidates for this, according to the authors' experiences in studying vibrations of a circular plate with V-notch [14]. Kim and Jung [15] also applied this methodology to investigate the vibrations of rhombic plates with V-notches. However, this work will demonstrate that using Williams' asymptotic solutions and regular polynomials as admissible functions does not yield quickly convergent solutions for a plate with a large side crack.

To remedy the mentioned problem, the present work proposes another set of functions to replace the corner functions to accelerate better the convergence of the numerical solutions. This set of functions is similar to the corner functions and also appropriately describes the behaviors of stress singularities at the crack tip and show the discontinuities of displacement and slope crossing the crack, which are characteristics of a true solution. The advantages of the proposed set of functions over the set of corner functions are demonstrated through comprehensive convergence studies for natural frequencies of a simply supported rectangular plate having a horizontal side crack with different lengths. The present numerical results are compared with the published results and show better accuracy than those obtained by the Ritz method combining with different domain

decomposition techniques (i.e., Refs. [11,12]). Finally, the present approach is applied to investigate the effects of location, length and orientation of side crack on the vibration behavior of a simply supported or a completely free square plate with a side crack. Numerical results are presented for the frequencies and nodal patterns, most of which have not been seen in the previous literature.

2. Methodology

The plate under consideration is a rectangular plate with a side crack as shown in Fig. 1. The well-known Ritz method is applied to determine the natural frequencies of such plate based on the classical plate theory. In the Ritz method, the maximum strain energy ($V_{\max}$) and the maximum kinetic energy ($T_{\max}$) for a plate vibrating harmonically with amplitude $W(x,y)$ and circular frequency ω are

$$V_{\max} = \frac{D}{2}\int\int_A (W_{,xx} + W_{,yy})^2 - 2(1-\upsilon)(W_{,xx}W_{,yy} - (W_{,xy})^2)\,\mathrm{d}A, \tag{1a}$$

$$T_{\max} = \frac{\omega^2 \rho h}{2}\int\int_A W^2\,\mathrm{d}A, \tag{1b}$$

where D, υ, h, and ρ are the flexural rigidity of the plate, Poisson's ratio, plate thickness, and mass per unit volume, respectively; and the subscript comma denotes partial differentiation with respect to the coordinate defined by the variable after the comma. The vibration frequencies of the plate are obtained by minimizing the energy functional

$$\Pi = V_{\max} - T_{\max}. \tag{2}$$

The admissible functions of the Ritz method have to satisfy the essential boundary conditions (or geometric boundary conditions) of the problem under consideration. For a rectangular plate with a side crack as shown in Fig. 1, the admissible functions for the transverse displacement are assumed as the sum of two sets of functions:

$$W(x,y) = x^{\bar{l}}y^{\bar{m}}(x-a)^{\bar{n}}(y-b)^{\bar{q}}[W_p(x,y) + W_c(r,\theta)], \tag{3}$$

where the function before the brackets is inserted to satisfy the geometric boundary conditions along $x=0$, $x=a$, $y=0$, and $y=b$; $W_p(x,y)$ consists of algebraic polynomials and is expressed as

$$\sum_{i=1,2}^{I}\sum_{j=1,2}^{J} a_{ij}x^{i-1}y^{j-1}, \tag{4}$$

which forms a mathematically complete set of functions if an infinite number of terms are used; $W_c(r,\theta)$ is used to supplement $W_p(x,y)$ appropriately describing the important behaviors of the true solutions of $W(x,y)$.

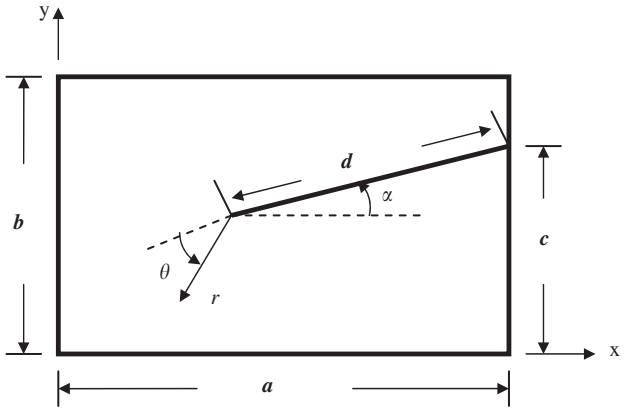

Fig. 1. Dimensions and coordinates for a side-cracked plate.

When considering the vibrations of a rectangular plate with a side crack, one easily sees that the true solutions should have the following properties: (a) proper stress singularities at the crack tip, (b) discontinuities of displacement and slope across the crack. Obviously, these properties cannot be accurately described by $W_p(x,y)$ in Eq. (4). Since a side crack can be treated as a special case of V-notch, Williams' asymptotic solutions [13] seem to be good candidates for $W_c(r,\theta)$ according to the authors' experiences [14].

Following the solution procedure given in Williams [13], one can find the asymptotic solutions (i.e., corner functions) for a crack with free boundary conditions along its two sides,

$$W_{nS}(r,\theta) = r^{\lambda_n+1}\left[\frac{\lambda_n(1-\upsilon)+3+\upsilon}{(\lambda_n+1)(\upsilon-1)}\cos(\lambda_n+1)\theta+\cos(\lambda_n-1)\theta\right], \tag{5a}$$

$$W_{nA}(r,\theta) = r^{\lambda_n+1}\left[-\frac{-\lambda_n(1-\upsilon)+3+\upsilon}{(\lambda_n+1)(\upsilon-1)}\sin(\lambda_n+1)\theta+\sin(\lambda_n-1)\theta\right], \tag{5b}$$

where W_{nS} and W_{nA} are symmetric and antisymmetric corner functions, respectively; the (r,θ) coordinate system is defined as shown in Fig. 1, its origin at the tip of crack, and $-\pi\leqslant\theta\leqslant\pi$; λ_n is the characteristic value of Willliams' asymptotic solution. In Eqs. (5), $\lambda_n=(2n-1)/2$ and $n=1,2,3,\ldots$. These corner functions accurately describe the singular behaviors near the tip of the crack and also satisfy the natural boundary conditions (namely, zero moment and effective shear force along the crack). Consequently, one can set

$$W_c(r,\theta) = \sum_{n=1,2}^{N_1} b_n W_{nS}(r,\theta) + \sum_{n=1,2}^{N_2} c_n W_{nA}(r,\theta), \tag{6}$$

where b_n and c_n are arbitrary constants. Notably, in Williams' original asymptotic solutions, λ_n can be an integer. However, integer λ_n are not used here because the resulting corner functions can be exactly expanded by finite terms of polynomials, which are already present in Eq. (4).

Another set of functions is also proposed for $W_c(r,\theta)$ herein, namely,

$$W_c(r,\theta) = \sum_{n=1}^{\overline{N}_1}\sum_{l=0}^{n} B_{nl} r^{(2n+1)/2}\cos\frac{2l+1}{2}\theta + \sum_{n=1}^{\overline{N}_2}\sum_{l=0}^{n} C_{nl} r^{(2n+1)/2}\sin\frac{2l+1}{2}\theta. \tag{7}$$

The purpose to propose Eq. (7) is to remedy certain shortcomings resulting from using Eqs. (5) and (6), which will become clear in Section 3 of this work. Notably, $W_c(r,\theta)$ in Eqs. (6) and (7) are linear combinations of the following two sets of functions, respectively,

$$\left\{r^{(2n+1)/2}\cos\left|\frac{2l+1}{2}\right|\theta \text{ and } r^{(2n+1)/2}\sin\left|\frac{2l+1}{2}\right|\theta \middle| l=n \text{ or } l=n-2 \text{ and } n=1,2,3,\ldots\right\}, \tag{8}$$

$$\left\{r^{(2n+1)/2}\cos\left|\frac{2l+1}{2}\right|\theta \text{ and } r^{(2n+1)/2}\sin\left|\frac{2l+1}{2}\right|\theta \middle| l=0,1,2,\ldots,n \text{ and } n=1,2,3,\ldots\right\}. \tag{9}$$

Comparison of Eqs. (8) and (9) reveals that the set of functions in Eq. (9) includes that of Eq. (8). Because λ_n in Eqs. (5) and $(2l+1)/2$ in Eq. (7) are not integers, the sine terms in these equations are not continuous at $\theta=\pm\pi$, while the cosine terms yield a discontinuity of circumferential slope $(\partial W_c/\partial\theta)$ at $\theta=\pm\pi$.

For simplicity, N_1 and N_2 in Eq. (6) are set equal to N, and $\overline{N}_1$ and $\overline{N}_2$ in Eq. (7) are set equal to $\overline{N}$ in the following computations. Substituting Eqs. (3)–(6) into Eqs. (1) and (2) and minimizing the functional Π with respect to undetermined coefficients a_{ij}, b_n and c_n yields IJ + 2N linear algebraic equations for those undetermined coefficients, which results in an eigenvalue problem with the eigenvalues related to the natural frequencies of plate. Similarly, utilizing Eq. (7), instead of Eqs. (5) and (6), in the above procedure yields $\mathrm{IJ}+\overline{N}(\overline{N}+3)$ linear algebraic equations for undetermined coefficients a_{ij}, B_{nl} and C_{nl}.

To accurately solve the eigenvalue problem, variables with 128-bit precision (with approximately 34 decimal digit accuracy) were used in the developed computer programs. Computations with 128-bit precision can be carried out using a regular PC with 64-bit operation system. The integrations needed in establishing solutions were carried out using the subroutine "DTWODQ" in IMSL Library, which was converted to 128-bit

precision from 64-bit precision. This subroutine uses the Gauss quadrature integration scheme proposed by Piessens et al. [16].

3. Convergence studies

Because infinite terms of admissible functions form a mathematically complete set of functions, the Ritz method yields solutions which converge to the exact solution from above as the number of admissible functions is sufficiently large. Convergence studies were carried out for simply supported rectangular plates with different crack lengths to verify the correctness of the solutions and demonstrate the effects of W_c on the solutions. In Eq. (3) $\overline{l},\overline{m},\overline{n}$, and $\overline{q}$ are set equal one to satisfy the geometric boundary conditions (zero transverse displacement) along simply supported edges. The rectangular plates have side length ratio $a/b = 2$ and a horizontal side crack at $c/b = 0.5$ with different crack lengths (d), where a, b, c, and d are defined in Fig. 1. Numerical results are presented for the first five nondimensional frequency parameters $\omega a^2\sqrt{\rho h/D}$. Poisson's ratio equal to 0.3 is considered for all the results shown here.

Tables 1–3 show the convergence studies of nondimensional frequency parameters for plates with crack length $d/a = 0.2$, 0.5 and 0.8, respectively. Corner functions given in Eqs. (5) and (6) were used for $W_c(r,\theta)$. In the first column of these tables parenthesized S and A denote symmetric and anti-symmetric modes, respectively. These tables also list the published results by Stahl and Keer [3], Yuan and Dickinson [11], or Liew et al. [12]. It should be noted that Stahl and Keer [3] used a very accurate Fredholm integration approach. Yuan and Dickinson [11] took the advantages of the symmetry of problem and analyzed a half of

Table 1
Convergence of frequency parameters $\omega a^2\sqrt{\rho h/D}$ for a simply supported rectangular plate having a central ($c/b = 0.5$) side crack with $d/a = 0.2$ (using W_c defined by Eqs. (5) and (6)).

Mode no.	N in W_c	Order of polynomial ($I \times J$)						Published results
		4×4	5×5	6×6	7×7	8×8	9×9	
1(S)	0	49.36[a]	49.35[a]	49.35[a]	49.35	49.35	49.35	[49.0]
	1	49.10[a]	49.03[a]	49.03	49.00	49.00	48.99	{49.04}
	3	49.02[a]	49.00[a]	49.00	48.99	48.99	48.98	(49.05)
	6	49.01[a]	49.00[a]	48.99	48.98	48.98	48.98	
2(S)	0	79.07[a]	79.06[a]	78.96[a]	78.96	78.96	78.96	[77.87]
	1	78.33[a]	78.14[a]	78.01	77.94	77.94	77.91	{78.04}
	3	78.13[a]	78.03[a]	77.93	77.90	77.90	77.89	(78.08)
	6	78.11[a]	77.94[a]	77.93	77.90	77.90	77.89	
3(S)	0	164.3[a]	129.5[a]	129.5[a]	128.3	128.3	128.3	[126.6]
	1	160.4[a]	127.9[a]	127.9	126.7	126.7	126.6	{126.8}
	3	134.0[a]	127.9[a]	127.8	126.6	126.6	126.6	(126.9)
	6	133.6[a]	126.8[a]	126.8	126.6	126.6	126.6	
4(A)	0	168.4[a]	168.4[a]	167.8[a]	167.8	167.8	167.8	[167.1]
	1	168.1[a]	168.1[a]	167.4	167.4	167.4	167.4	{167.2}
	3	167.7[a]	167.7[a]	167.1	167.1	167.1	167.1	(167.2)
	6	167.7[a]	167.2[a]	167.1	167.1	167.1	167.1	
5(A)	0	198.0[a]	198.0[a]	197.4[a]	197.4	197.4	197.4	[194.0]
	1	196.5[a]	196.2[a]	195.6	195.6	195.5	195.4	{194.4}
	3	194.7[a]	194.7[a]	194.2	194.2	194.2	194.2	(194.7)
	6	194.7[a]	194.6[a]	194.2	194.2	194.2	194.2	

Note: []: results from Stahl and Keer [3]; {}: results from Yuan and Dickinson [11]; and (): results from Liew et al. [12].
[a]Computations with 64-bit precision were used.

Table 2
Convergence of frequency parameters $\omega a^2\sqrt{\rho h/D}$ for a simply supported rectangular plate having a central ($c/b = 0.5$) side crack with $d/a = 0.5$ (using W_c defined by Eqs. (5) and (6)).

Mode no.	N in W_c	Order of polynomial ($I \times J$)						Published results
		4×4	5×5	6×6	7×7	8×8	9×9	
1(S)	0	49.36	49.35	49.35	49.35	49.35	49.35	[40.4]
	5	40.88	40.61	40.60	40.47	40.47	40.42	{41.27}
	10	40.87	40.61	40.58	40.47	40.47	40.42	(41.62)
	15	40.87	40.61	40.58	40.47	40.47	40.42	
	20	40.87	40.61	40.58	40.47	40.47	40.42	
2(S)	0	79.07	79.06	78.96	78.96	78.96	78.96	[72.79]
	5	73.25	72.95	72.94	72.86	72.86	72.82	{72.79}
	10	73.22	72.94	72.92	72.86	72.85	72.82	(72.89)
	15	73.22	72.94	72.92	72.86	72.85	72.82	
	20	73.21	72.94	72.92	72.86	72.85	72.82	
3(A)	0	164.3	129.5	129.5	128.3	128.3	128.3	[73.63]
	5	76.92	76.87	76.26	76.26	75.77	75.76	{74.63}
	10	76.87	76.69	76.25	76.11	75.75	75.65	(76.55)
	15	76.87	76.68	76.25	76.10	75.74	75.63	
	20	76.87	76.68	76.25	76.10	75.74	75.63	
4(S)	0	168.4	168.4	167.8	167.8	167.8	167.8	[123.4]
	5	130.0	124.7	123.8	123.5	123.5	123.5	{123.8}
	10	129.9	123.9	123.7	123.5	123.5	123.5	(123.8)
	15	129.9	123.9	123.7	123.5	123.5	123.5	
	20	129.9	123.9	123.7	123.5	123.5	123.5	
5(A)	0	198.0	198.0	197.4	197.4	197.4	197.4	[168.6]
	5	170.3	169.7	169.5	169.4	169.3	169.3	{169.7}
	10	170.1	169.6	169.3	169.3	169.3	169.3	(170.5)
	15	170.1	169.6	169.3	169.3	169.3	169.3	
	20	170.1	169.6	169.3	169.3	169.3	169.3	

Note: []: results from Stahl and Keer [3]; {}: results from Yuan and Dickinson [11]; and (): results from Liew et al. [12].

plate only. They decomposed the domain under consideration into two subdomains and used 8×8 terms of orthogonal polynomials for each subdomain to construct the solution. Similar to the approach by Yuan and Dickinson [11], Liew et al. [12] used 19×9 terms of orthogonal polynomials for each subdomain. As mentioned in the Introduction (Section 1), the solutions of Yuan and Dickinson [11] and Liew et al. [12] are not guaranteed to be the upper bounds of true solutions.

In Table 1, the results with superscript "a" were obtained by using 64-bit precision in computations. When computations with 64-bit precision were performed, using more than 7×7 terms of polynomials with no corner functions in the admissible functions yields ill-conditioned matrixes. Ill-conditioned matrixes also occur when 6×6 terms of polynomials with any corner functions were used. Computations with 128-bit precision allow using a larger number of terms in admissible functions before ill-conditioned matrixes occur. Notably, computations with these two different precisions yield identical solutions up to at least six significant figures when the same admissible functions are used and numerical instability does not occur.

Tables 1–3 disclose several interesting facts. Carefully examining the results with no $W_c(r,\theta)$ ($N = 0$) in Table 1, one finds that the numerical results converge to the exact results for a simply supported intact

Table 3
Convergence of frequency parameters $\omega a^2\sqrt{\rho h/D}$ for a simply supported rectangular plate having a central ($c/b = 0.5$) side crack with $d/a = 0.8$ (using W_c defined by Eqs. (5) and (6)).

Mode no.	N in W_c	Order of polynomial ($I \times J$)						Published results
		4×4	5×5	6×6	7×7	8×8	9×9	
1(S)	0	49.36	49.35	49.35	49.35	49.35	49.35	[29.9]
	5	31.30	30.48	30.47	30.15	30.15	30.03	(30.50)
	10	31.28	30.47	30.46	30.15	30.15	30.03	
	15	31.27	30.47	30.46	30.15	30.15	30.03	
	20	31.27	30.47	30.45	30.15	30.15	30.03	
2(A)	0	79.07	79.06	78.96	78.96	78.96	78.96	[39.53]
	5	44.83	44.81	43.49	43.48	42.68	42.68	(40.02)
	10	44.80	44.79	43.48	43.48	42.67	42.66	
	15	44.80	44.79	43.48	43.47	42.66	42.66	
	20	44.80	44.79	43.47	42.66	42.66	42.65	
3(S)	0	164.3	129.5	129.5	128.3	128.3	128.3	[68.20]
	5	68.78	68.44	68.44	68.33	68.33	68.27	(68.82)
	10	68.75	68.44	68.42	68.33	68.32	68.27	
	15	68.74	68.44	68.42	68.33	68.32	68.27	
	20	68.74	68.44	68.42	68.33	68.32	68.27	
4(A)	0	168.4	168.4	167.8	167.8	167.8	167.8	[94.50]
	5	96.77	96.64	96.40	96.39	96.09	96.09	(95.79)
	10	96.72	96.59	96.35	96.32	96.03	96.03	
	15	96.72	96.58	96.35	96.32	96.02	96.02	
	20	96.72	96.58	96.35	96.02	96.02	96.01	
5(S)	0	198.0	198.0	197.4	197.4	197.4	197.4	[120.2]
	5	143.1	121.7	121.3	120.3	120.3	120.2	(120.3)
	10	141.7	121.1	120.6	120.3	120.3	120.2	
	15	141.2	121.1	120.6	120.3	120.3	120.2	
	20	140.9	121.0	120.6	120.3	120.3	120.2	

Note: [ ]: results from Stahl and Keer [3] and ( ): results from Liew et al. [12].

rectangular plate [1]; that is, integer multiplies of π^2. This observation is expected because existence of the side crack cannot be recognized by the polynomial admissible functions (Eq. (4)) alone. Adding a small number of terms in $W_c(r,\theta)$ into the admissible functions significantly improves numerical solutions. Table 1 demonstrates that the numerical solutions converge very well for the case with a small crack ($d/a = 0.2$). Using $I = J = 7$ and $N = 3$ (totally 55 terms) in the admissible function leads to at least three significant figure convergence, and the convergent results show excellent agreement with those of Stahl and Keer [3]. The results obtained by Yuan and Dickinson [11] and Liew et al. [12] are less accurate.

It should be noted that Stahl and Keer [3] gave the first frequency to only three significant figures. Their solution required discretization of their integral equation. Consequently, they admitted that the fourth significant figure of their other results "may not be accurate".

Table 2 shows that the convergence of results for the deeper crack ($c/b = 0.5$) is not so good as that found in Table 1. Using the results of Stahl and Keer [3] as a comparison basis, the present upper bound results obtained by using $I = J = 9$ and $N = 15$ (totally 121 terms) in admissible functions are all better than those given by Liew et al. [12] and are better than those obtained by Yuan and Dickinson [11] for the first, fourth

Table 4
Convergence of frequency parameters $\omega a^2\sqrt{\rho h/D}$ for the same case as Table 1, but using W_c defined by Eq. (7).

Mode no.	$\overline{N}$ in W_c	Order of polynomial ($I\times J$)					Published results
		4×4	5×5	6×6	7×7	8×8	
1(S)	2	49.01	48.98	48.98	48.97	48.97	[49.0]
	3	48.97	48.97	48.97	48.97	48.97	{49.04}
	4	48.97	48.97	48.97	48.97	48.97	(49.05)
2(S)	2	78.01	77.96	77.88	77.87	77.87	[77.87]
	3	77.96	77.87	77.87	77.87	77.87	{78.04}
	4	77.87	77.87	77.87	77.87	77.87	(78.08)
3(S)	2	129.4	127.3	127.3	126.6	126.6	[126.6]
	3	127.3	127.3	126.8	126.6	126.6	{126.8}
	4	127.3	126.8	126.6	126.6	126.6	(126.9)
4(A)	2	167.5	167.5	167.1	167.1	167.1	[167.1]
	3	167.2	167.2	167.1	167.1	167.1	{167.2}
	4	167.1	167.1	167.1	167.1	167.1	(167.2)
5(A)	2	194.5	194.5	194.1	194.1	194.1	[194.0]
	3	194.4	194.4	194.0	194.0	194.0	{194.4}
	4	194.1	194.1	194.0	194.0	194.0	(194.7)

Note: []: results from Stahl and Keer [3]; { }: results from Yuan and Dickinson[11]; and ( ): results from Liew et al. [12].

and fifth modes. Nevertheless, the agreement of the present results with those of Stahl and Keer is not so impressive, especially for the third mode.

Table 3 displays that the convergence of the results for the deepest crack ($c/b = 0.8$) is even slower than that shown in Table 2. Although the results obtained by using $I = J = 9$ and $N = 20$ (totally 131 terms) in admissible functions are less than those of Liew et al. [12] in the first, third and fifth modes, these results are still significantly larger than those of Stahl and Keer [3].

Using more terms than those shown in Tables 2 and 3 easily causes ill-conditioned matrices in the process of computation. Moreover, when carefully examining the eigenvector components of the first five modes of the present results, one finds that the eigenvector components corresponding to higher orders of r in W_c (say, larger than 10) are remarkably smaller than those corresponding to lower orders of r. Intuitively, Eq. (7) was proposed because the set of functions in Eq. (9) includes that of Eq. (8), and Eq. (7) has $\hat{N}(\hat{N}+3)$ terms with orders of r less than (or equal to) $(2\hat{N}+1)/2$ while Eq. (6) only has $2\hat{N}$ terms.

Similar to the presentation in Tables 1–3, Tables 4–6 illustrate the corresponding convergence studies by using $W_c(r,\theta)$ defined in Eq. (7). Recall that adding $W_c(r,\theta)$ defined by Eq. (6) or Eq. (7) into the admissible functions always yields upper-bound solutions for natural frequencies. Eq. (7) gives significantly better results than Eq. (6) does for the cases of $d/a = 0.5$ and 0.8 if same number of terms are used for $W_c(r,\theta)$. This fact can be observed by comparing the results in Tables 5 and 6 obtained by using $\overline{N} = 5$ with those in Tables 2 and 3 with $N = 20$, respectively. Notably, $\overline{N} = 5$ and $N = 20$ yield 40 terms in Eqs. (7) and (6), respectively. The resulting eigenvalue determinants to be evaluated are then of order $40+\mathrm{IJ}$. Comparison of the results in Tables 1 and 4 discloses that Eq. (7) does not give significantly better results than Eq. (6) does because Eq. (6) already provides excellent convergent solutions in the case of small crack ($d/a = 0.2$). Using Eq. (7) for the admissible functions otherwise considerably accelerates the convergence of the numerical results, and the convergent results in Tables 4–6 agree excellently with those of Stahl and Keer [3].

Table 5
Convergence of frequency parameters $\omega a^2\sqrt{\rho h/D}$ for the same case as Table 2, but using W_c defined by Eq. (7).

Mode no.	$\overline{N}$ in W_c	Order of polynomial ($I \times J$)					Published results
		4×4	5×5	6×6	7×7	8×8	
1(S)	3	40.43	40.36	40.36	40.36	40.36	[40.4]
	4	40.39	40.36	40.36	40.35	40.35	{41.27}
	5	40.38	40.35	40.35	40.35	40.35	(41.62)
	6	40.37	40.35	40.35	40.35	40.35	
	7	40.36	40.35	40.35	40.35	40.35	
2(S)	3	72.92	72.80	72.79	72.78	72.78	[72.79]
	4	72.85	72.78	72.78	72.78	72.78	{72.79}
	5	72.83	72.78	72.78	72.78	72.78	(72.89)
	6	72.82	72.78	72.78	72.78	72.78	
	7	72.82	72.78	72.78	72.78	72.78	
3(A)	3	73.73	73.72	73.67	73.66	73.65	[73.63]
	4	73.64	73.64	73.63	73.63	73.63	{74.63}
	5	73.64	73.64	73.63	73.63	73.63	(76.55)
	6	73.63	73.63	73.63	73.63	73.63	
	7	73.63	73.63	73.63	73.63	73.63	
4(S)	3	124.0	123.8	123.7	123.5	123.5	[123.4]
	4	123.7	123.6	123.5	123.4	123.4	{123.8}
	5	123.6	123.5	123.4	123.4	123.4	(123.8)
	6	123.5	123.5	123.4	123.4	123.4	
	7	123.5	123.5	123.4	123.4	123.4	
5(A)	3	169.8	169.5	169.2	169.2	169.0	[168.6]
	4	169.0	169.0	169.0	168.9	168.9	{169.7}
	5	168.9	168.9	168.9	168.9	168.9	(170.5)
	6	168.9	168.9	168.9	168.9	168.9	
	7	168.9	168.9	168.9	168.9	168.9	

Note: [ ]: results from Stahl and Keer [3]; { }: results from Yuan and Dickinson [11]; and ( ): results from Liew et al. [12].

4. Numerical results and discussion

After Eqs. (4) and (7) as admissible functions have been demonstrated to yield excellently convergent solutions for a simply supported rectangular plate with a side crack, they were further applied to investigate the vibration behaviors of simply supported and completely free square plates with side cracks at different locations ($c/b = 0.5$ and 0.75) with various lengths ($d/a = 0.1$ to 0.6) and orientations ($\alpha = 0^\circ$, 15°, and 30°). In Eq. (3) $\overline{l}, \overline{m}, \overline{n}$, and $\overline{q}$ are set equal zero when a completely free plate is considered, for there are no geometric boundary conditions then. Tables 7 and 8 display the nondimensional frequency parameters for the first five nonzero frequency modes for simply supported and completely free square plates, respectively. Poisson's ratio is set equal to 0.3. The results for $d/a \leqslant 0.3$ were obtained by using 7×7 terms of polynomials along with $\overline{N} = 5$ in $W_c(r,\theta)$, which results in 89 admissible functions totally; while the results for $d/a \geqslant 0.4$ were obtained by using 8×8 terms of polynomials and $\overline{N} = 6$ in $W_c(r,\theta)$, which results in 118 functions totally. Other studies not shown here indicate that the results have converged to at least 3-digit accuracy.

Looking first at the simply supported square plates (Table 7), one may begin by noting that the exact values [1] of the first five frequency parameters with no crack are 19.74, 49.35, 49.35, 78.96 and 98.70 ($n\pi^2$, with $n = 2$, 5, 5, 8, 10). It is seen that adding a small crack ($d/a = 0.1$) causes very little change in any of the first five frequencies. As expected, increasing crack length (d/a) results in decreasing frequencies, for all modes.

Table 6
Convergence of frequency parameters $\omega a^2\sqrt{\rho h/D}$ for the same case as Table 3, but using W_c defined by Eq. (7).

Mode no.	$\overline{N}$ in W_c	Order of polynomial ($I \times J$)					Published results
		4×4	5×5	6×6	7×7	8×8	
1(S)	3	30.08	29.94	29.94	29.92	29.92	[29.9]
	4	29.99	29.91	29.91	29.90	29.90	(30.50)
	5	29.96	29.91	29.90	29.90	29.90	
	6	29.94	29.91	29.90	29.90	29.90	
	7	29.94	29.91	29.90	29.90	29.90	
	8	29.94	29.91	29.90	29.90	29.90	
2(A)	3	39.92	39.88	39.84	39.84	39.82	[39.53]
	4	39.69	39.65	39.62	39.62	39.62	(40.02)
	5	39.59	39.58	39.57	39.56	39.56	
	6	39.57	39.56	39.55	39.55	39.55	
	7	39.56	39.55	39.55	39.55	39.54	
	8	39.56	39.55	39.54	39.54	39.54	
3(S)	3	68.66	68.28	68.27	68.25	68.25	[68.20]
	4	68.49	68.24	68.23	68.22	68.22	(68.82)
	5	68.38	68.22	68.21	68.21	68.21	
	6	68.36	68.22	68.21	68.21	68.21	
	7	68.34	68.22	68.21	68.21	68.21	
	8	68.33	68.21	68.21	68.21	68.21	
4(A)	3	96.66	96.38	95.85	95.80	95.69	[94.50]
	4	94.87	94.70	94.66	94.66	94.64	(95.79)
	5	94.63	94.62	94.59	94.59	94.59	
	6	94.57	94.56	94.56	94.55	94.54	
	7	94.54	94.54	94.53	94.53	94.53	
	8	94.53	94.53	94.53	94.53	94.52	
5(S)	3	133.7	122.8	122.5	121.9	121.9	[120.2]
	4	132.0	121.4	120.4	120.2	120.2	(120.3)
	5	131.7	121.0	120.4	120.2	120.2	
	6	131.4	120.8	120.3	120.2	120.2	
	7	131.3	120.8	120.3	120.2	120.2	
	8	131.3	120.8	120.3	120.2	120.2	

Note: []: results from Stahl and Keer [3] and ( ): results from Liew et al. [12].

For plates with centrally located cracks, parallel to the edges, the free vibration mode shapes are either symmetric or antisymmetric to one axis ($y = b/2$) of the plate. This is seen in the nodal patterns (lines of zero displacement) shown in Fig. 2 when $\alpha = 0^\circ$ and $c/b = 0.5$. In this case all modes are symmetric (e.g., modes 1, 2 and 5) or antisymmetric (e.g., modes 3 and 4) with respect to that plate axis. For the relatively short crack ($d/a = 0.2$) the node lines seen in Fig. 2 for the first four modes are almost identical to those of the plate with no crack. The difference shows up more clearly for mode 5, where the two diagonal node lines, which are perfectly straight with no crack, are distorted significantly.

When the crack is not at the center (e.g., $c/b = 0.75$), Table 7 shows that the frequencies can be either more or less affected by it, depending upon the modes. An off-center crack completely destroys any symmetry, as may be seen in the lack of symmetry in the node lines of Fig. 2 (for example, with $\alpha = 0^\circ$, $c/b = 0.75$). For $\alpha \neq 0^\circ$, Fig. 2 shows that the otherwise symmetrical node lines are further distorted. It is

Table 7
Frequency parameters $\omega a^2\sqrt{\rho h/D}$ for simply supported square plates with side cracks at various orientations (α), locations (c/b) and lengths (d/a).

α (degrees)	c/b	d/a	Mode				
			1	2	3	4	5
0	0.5	0.1	19.74	49.34	49.35	78.95	98.63
		0.2	19.70	49.19	49.33	78.78	97.88
		0.3	19.54	48.77	49.09	77.18	95.69
		0.4	19.20	47.80	48.24	71.27	92.23
		0.5	18.65	43.42	47.92	64.40	88.08
		0.6	17.96	36.45	47.86	62.24	83.78
0	0.75	0.1	19.74	49.33	49.35	78.91	98.67
		0.2	19.72	49.08	49.34	78.40	98.30
		0.3	19.62	48.15	49.23	76.96	96.95
		0.4	19.38	46.34	48.74	75.18	87.28
		0.5	18.88	44.07	47.32	68.85	76.03
		0.6	18.10	41.65	44.52	58.84	75.30
15	0.75	0.1	19.73	49.32	49.35	78.92	98.66
		0.2	19.68	49.04	49.34	78.50	98.36
		0.3	19.51	48.24	49.29	77.23	97.17
		0.4	19.15	46.97	48.88	74.82	86.37
		0.5	18.56	45.47	47.09	65.76	77.42
		0.6	17.79	40.54	45.61	58.76	76.03
30	0.75	0.1	19.72	49.31	49.35	78.94	98.61
		0.2	19.64	49.03	49.35	78.69	98.03
		0.3	19.44	48.33	49.30	77.78	96.12
		0.4	19.07	47.39	48.89	75.12	87.14
		0.5	18.50	46.50	46.67	66.22	79.56
		0.6	17.78	39.99	46.38	60.77	77.66

also interesting to note in Fig. 2 that node lines may intersect a crack and, in some cases, even the tip of a crack.

Considering next the completely free square plate, nondimensional frequencies are given in Table 8, and corresponding nodal patterns are shown in Fig. 3. Because the nodal patterns for the free plate with no crack are less obvious than those of the simply supported one, they are shown additionally in the first row ($d/a = 0$) of Fig. 3. Notably, the first five nonzero nondimensional frequency parameters for a completely free intact square plate are 13.47, 19.61, 24.28, 34.82, 34.82 [17]. The authors know of no other published frequencies or nodal patterns for free square plates with cracks.

Comparing Tables 7 and 8, one sees that the presence of an edge crack affects the fundamental (i.e., lowest) frequency of the free plate much more than that of the simply supported one. The fundamental mode shape of the free plate with no crack is antisymmetric, whereas for the simply supported one it is symmetric. But this effect does not extend to the other modes of the plates; that is, symmetric mode frequencies in some cases are more greatly affected by a crack than the antisymmetric modes.

5. Concluding remarks

This paper has illustrated a novel Ritz method to accurately determine the natural frequencies of a rectangular plate with a side crack. A new set of functions has been proposed to supplement the regular

Table 8
Frequency parameters $\omega a^2\sqrt{\rho h/D}$ for a completely free square plate with a side crack.

α (degrees)	c/b	d/a	Mode				
			1	2	3	4	5
0	0.5	0.1	13.31	19.41	24.08	34.19	34.24
		0.2	12.72	18.83	23.55	32.07	33.13
		0.3	11.58	17.77	22.89	28.48	32.30
		0.4	9.956	16.35	22.35	25.16	31.95
		0.5	8.249	14.77	21.97	23.10	31.90
		0.6	6.761	13.22	21.74	21.82	31.87
0	0.75	0.1	13.36	19.53	24.20	34.20	34.66
		0.2	12.97	19.25	23.87	31.60	34.31
		0.3	12.11	18.43	22.83	27.75	33.92
		0.4	10.56	16.79	21.59	25.91	33.57
		0.5	8.642	15.30	21.10	25.06	33.23
		0.6	6.922	14.25	20.95	24.25	32.65
15	0.75	0.1	13.36	19.51	24.20	34.22	34.63
		0.2	12.97	19.11	23.85	31.81	34.15
		0.3	12.14	17.92	23.07	28.20	33.57
		0.4	10.70	15.92	22.36	25.94	33.13
		0.5	8.902	14.19	22.04	24.61	32.84
		0.6	7.239	12.86	21.85	23.54	32.32
30	0.75	0.1	13.38	19.51	24.20	34.31	34.63
		0.2	13.04	19.06	23.87	32.29	34.04
		0.3	12.35	17.68	23.24	28.95	33.28
		0.4	11.12	15.45	22.67	26.37	32.69
		0.5	9.384	13.59	22.18	24.85	32.36
		0.6	7.650	12.23	21.50	24.06	32.10

polynomial admissible functions in order to significantly accelerate the convergence of the numerical solutions from the upper-bound. The proposed set of functions appropriately describes the behaviors of stress singularities at the crack tip and shows the discontinuities of displacement and slope crossing the crack, which may be the characteristics of a true solution.

The effects of the proposed set of functions on determining the frequencies of a side-cracked plate have been comprehensively investigated through careful convergence studies for simply supported plates with horizontal side cracks having different crack lengths. The proposed set of functions demonstrates the superiority to the corner functions derived from Williams' solutions on improving the convergence of solutions, especially for a large crack. Furthermore, the present solutions show better accuracy than the previously published ones obtained by the Ritz method with different domain decomposition techniques.

Accurate frequencies and nodal patterns have been tabulated for simply supported and completely free square plates having side cracks at different locations ($c/b = 0.5$ and 0.75), with various lengths ($d/a = 0.1$ to 0.6) and orientations ($\alpha = 0^\circ$, 15°, and 30°). The shown frequencies are accurate to at least three significant figures. Most of these results are the first ones shown in the published literature.

Although only side-cracked rectangular plates with simply supported and completely free boundary conditions are considered, the present methodology can be applied to plates with other shapes and boundary conditions. It will be also interesting to extend the methodology with a simple modification to determine the stress intensity factors of a plate subjected to different loads.

α	c/b	d/a	Mode No.				
			1	2	3	4	5
0°	0.5	0.2	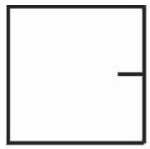		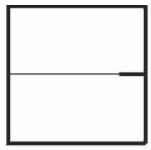	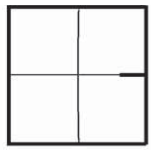	
		0.5	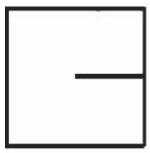	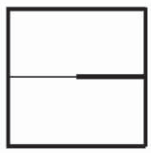	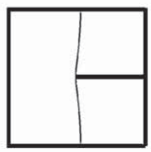		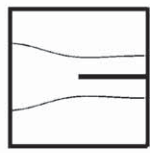
	0.75	0.2	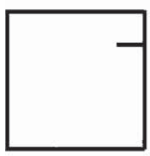	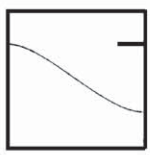		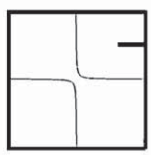	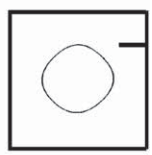
		0.5	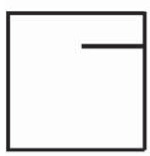			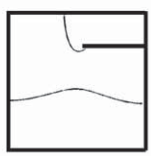	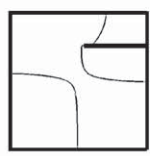
15°	0.75	0.2	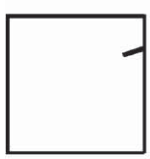			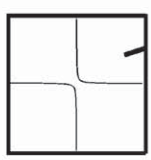	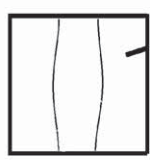
		0.5		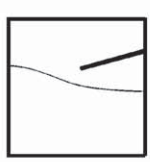			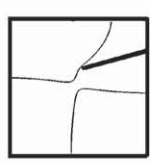
30°	0.75	0.2	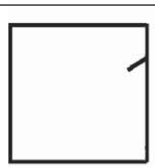	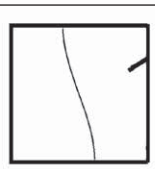		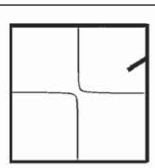	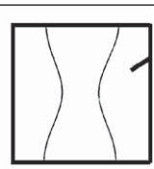
		0.5				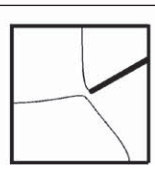	

Fig. 2. Nodal patterns for a simply supported square plate with a side crack.

α	c/b	d/a	Mode No.				
			1	2	3	4	5
		0	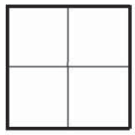	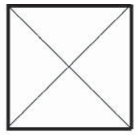	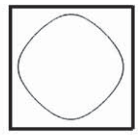	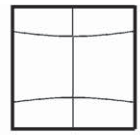	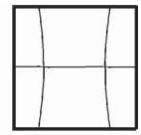
0°	0.5	0.2	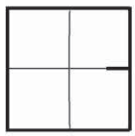		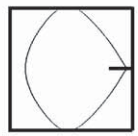	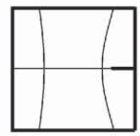	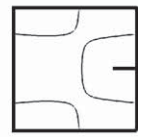
		0.5	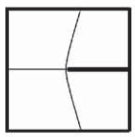	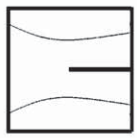	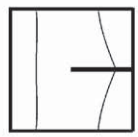	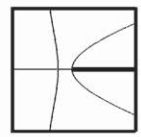	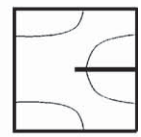
	0.75	0.2			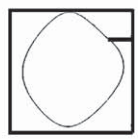		
		0.5		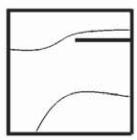			
15°	0.75	0.2	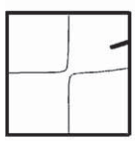		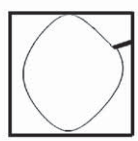		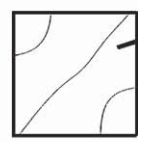
		0.5			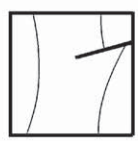		
30°	0.75	0.2	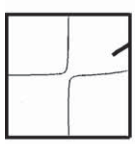		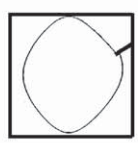		
		0.5					

Fig. 3. Nodal patterns for a completely free square plate with a side crack.

Acknowledgment

This work reported herein was supported by the National Science Council, Taiwan through research Grant no. NSC97-2221-E-009-075-MY3. This support is gratefully acknowledged.

References

[1] A.W. Leissa, *Vibration of Plates*, NASA SP-160, US Government Printing Office, 1969; Reprinted by The Acoustical Society of America, 1993.
[2] P.P. Lynn, N. Kumbasar, Free vibrations of thin rectangular plates having narrow cracks with simply supported edges, *Developments in Mechanics*, 4, *Proceedings of the 10th Midwestern Mechanics Conference*, Colorado State University, Fort Collins, CO, August 21–23, 1967, pp. 911–928.
[3] B. Stahl, L.M. Keer, Vibration and stability of cracked rectangular plates, *International Journal of Solids and Structures* 8 (1) (1972) 69–91.
[4] B.D. Aggarwala, P.D. Ariel, Vibration and bending of a cracked plate, *Rozprawy Inzynierskie* 29 (2) (1981) 295–310.
[5] K. Neku, Free vibration of a simply-supported rectangular plate with a straight through-notch, *Bulletin of the Japan Society of Mechanical Engineers* 25 (199) (1982) 16–23.
[6] R. Solecki, Bending vibration of a simply supported rectangular plate with a crack parallel to one edge, *Engineering Fracture Mechanics* 18 (6) (1983) 1111–1118.
[7] S.E. Khadem, M. Rezaee, Introduction of modified comparison functions for vibration analysis of a rectangular cracked plate, *Journal of Sound and Vibration* 236 (2) (2000) 245–258.
[8] Y. Hirano, K. Okazaki, Vibration of cracked rectangular plates, *Bulletin of the Japan Society of Mechanical Engineers* 23 (179) (1980) 732–740.
[9] G.L. Qian, S.N. Gu, J.S. Jiang, A finite element model of cracked plates and application to vibration problems, *Computers and Structures* 39 (5) (1991) 483–487.
[10] M. Krawczuk, Natural vibrations of rectangular plates with a through crack, *Archive of Applied Mechanics* 63 (7) (1993) 491–504.
[11] J. Yuan, S.M. Dickinson, The flexural vibration of rectangular plate systems approached by using artificial springs in the Rayleigh–Ritz method, *Journal of Sound and Vibration* 159 (1) (1992) 39–55.
[12] K.M. Liew, K.C. Hung, M.K. Lim, A solution method for analysis of cracked plates under vibration, *Engineering Fracture Mechanics* 48 (3) (1994) 393–404.
[13] M.L. Williams, Surface stress singularities resulting from various boundary conditions in angular corners of plates under bending, *Proceedings of the First US National Congress of Applied Mechanics*, 1952, pp. 325–329.
[14] A.W. Leissa, O.G. McGee, C.S. Huang, Vibrations of circular plates having V-notches or sharp radial cracks, *Journal of Sound and Vibration* 161 (2) (1993) 227–239.
[15] J.W. Kim, H.Y. Jung, Influence of stress singularities on the vibration of rhombic plates with V-notches or sharp cracks, *Key Engineering Materials* 270–273 (2004) 1414–1419.
[16] R. Piessens, E. deDoncker-Kapenga, C.W. Überhuber, D.K. Kahaner, *QUADPACK*, Springer, New York, 1983.
[17] C.P. Filipich, M.B. Rosales, Arbitrary precision frequencies of a free rectangular thin plate, *Journal of Sound and Vibration* 230 (3) (2000) 521–539.